https://doi.org/10.5194/acp-2020-596
Preprint. Discussion started: 6 August 2020

Atmospheric Chemistry and Physics Discussions
Open Access
EGU

Synoptic drivers of co-occurring summertime ozone and $PM_{2.5}$ pollution in eastern China

Lian Zong[1], Yuanjian Yang[1,*], Meng Gao[2], Hong Wang[1], Peng Wang[3], Hongliang Zhang[4], Linlin Wang[5], Guicai Ning[6], Chao Liu[1], Yubin Li[1], Zhiqiu Gao[1,5]

1. School of Atmospheric Physics, Nanjing University of Information Science & Technology, Nanjing, China
2. Department of Geography, Hong Kong Baptist University, Hong Kong SAR, China
3. Policy Research Center for Environment and Economy, Ministry of Ecology and Environment of the People's Republic of China, Beijing, China
4. Department of environmental science and engineering, Fudan University, China
5. State Key Laboratory of Atmospheric Boundary Layer Physics and Atmospheric Chemistry (LAPC), Institute of Atmospheric Physics, Chinese Academy of Sciences, Beijing, China
6. Institute of Environment, Energy and Sustainability, The Chinese University of Hong Kong, Shatin, N.T., Hong Kong, China

* Correspondence to: Dr./Prof. Y. Yang (yyj1985@nuist.edu.cn)

https://doi.org/10.5194/acp-2020-596
Preprint. Discussion started: 6 August 2020

Atmospheric Chemistry and Physics Discussions
Open Access
EGU

Abstract

In recent years, surface ozone (O_3) pollution during summertime (June-August) over eastern China has become more serious, and it is even the case that surface O_3 and $PM_{2.5}$ (particulate matter with aerodynamic diameter ≤ 2.5 μm in the air) pollution can co-occur. However, the synoptic circulation pattern related to this compound pollution remains unclear. In this study, the T-mode principal component analysis method is used to objectively classify four synoptic weather patterns (SWPs) that occur over eastern China, based on the geopotential heights at 500 hPa during summertime from 2015 to 2018. Four SWPs of eastern China are closely related to the western Pacific subtropical high (WPSH), exhibiting, significant intraseasonal and interannual variations. Note that remarkable spatial and temporal disparities of surface O_3 and $PM_{2.5}$ pollution are given under these four different SWPs according to the ground-level air quality and meteorological observations. In areas controlled by the WPSH or the prevailing westerlies, O_3 pollution is mainly caused by photochemical reactions of nitrogen oxides and volatile organic compounds under weather conditions of high temperature, moderate humidity and slight precipitation. In particular, the warm moist flow brought by the WPSH can promote hygroscopic growth of fine particulate matter in some local areas, resulting in the increase of $PM_{2.5}$ concentrations, which may form co-occurring surface O_3 and $PM_{2.5}$ pollution. In addition, the low boundary layer height and frequency of light-wind days are closely related to the transmission and diffusion of pollutants under the different SWPs, modulating the levels of O_3-$PM_{2.5}$ compound pollution. Overall, our findings demonstrate the different roles played by synoptic weather patterns in driving regional surface O_3-$PM_{2.5}$ compound pollution, in addition to the large quantities of emissions, and may also provide insights into the regional co-occurring high $PM_{2.5}$ and high O_3 level via the effects of certain meteorological factors.

Keywords: Synoptic weather pattern, ozone, $PM_{2.5}$, compound pollution, western Pacific subtropical high (WPSH)

1. Introduction

In recent years, China has been experiencing serious air pollution problems due to the

https://doi.org/10.5194/acp-2020-596
Preprint. Discussion started: 6 August 2020

enormous emissions of polluting gases [e.g., sulfur dioxide, nitrogen dioxide (NO_2), etc.] and aerosol particulates [e.g., particulate matter with aerodynamic diameter ≤ 2.5 (10) μm in the air $PM_{2.5}$ (PM_{10}), etc.] associated with its rapid economic development, industrialization and urbanization, together with certain unfavorable meteorological conditions (Wang & Chen, 2016; Zhang et al., 2014; Y. Zhang et al., 2016). Particularly, atmospheric compound pollution has become serious (Li et al., 2019; Saikawa et al., 2017; C. Zhang et al., 2019), especially for the economically developed and densely populated eastern urban agglomerations of China, such as the Beijing–Tianjin–Hebei (BTH), Yangtze River Delta (YRD) and Pearl River Delta (PRD) regions (Cai et al., 2017; Du et al., 2019; Ji et al., 2018; Li et al., 2020), exerting a severe threat in terms of public health, economy and society (Chen et al., 2019; Cohen et al., 2017; Day et al., 2017; Yim et al., 2019).

In general, $PM_{2.5}$ pollution is featured with obvious diurnal and seasonal changes. Due to the influence of atmospheric diffusion conditions such as precipitation and wind speed (WS), it tends to be enhanced in the morning and evening, lower at noon, and higher in winter and lower in summer (Amil et al., 2016; H. Liu et al., 2019; Ye et al., 2018; Zhang & Cao, 2015). The $PM_{2.5}$ level of China showed a steady increase from 2004 to 2007, and has since stabilized (Ma et al., 2016); however, there are still frequent $PM_{2.5}$ pollution events in autumn and winter (Song et al., 2017; Yang et al., 2018; Ye et al., 2018; Zhang et al., 2014). In the past few years, the $PM_{2.5}$ concentration in China has decreased significantly as a result of measures introduced across the country that have reduced multi-pollutant emissions, adjusted energy structure, and increased supply of clean energy (Gui et al., 2019; Yang et al., 2020; Q. Zhang et al., 2019; Zhang et al., 2020). In contrast, summer O_3 pollution has gradually been prominent, replacing $PM_{2.5}$ as the primary pollutant in the air (Li et al., 2019). As a secondary pollutant, ozone in the troposphere is mainly formed by photochemical reactions between NO_x, carbon monoxide (CO) and VOCs in the exposure of sunlight (Sillman, 2002). The prominent problem of O_3 pollution has attracted the attention of experts and scholars in recent years. For instance, Sun et al. (2016) showed that the observed summertime O_3 at Mt. Tai has increased significantly by 1.7 ppbv yr^{-1} for June and 2.1 ppbv yr^{-1} for July–August during the period of 2003 to 2015. An increase of the maximum daily 8-h average concentration of O_3 (MDA8 O_3) at an annual-average rate of 4.6%, was reported by Fan et al. (2020), albeit with a decrease of the

https://doi.org/10.5194/acp-2020-596
Preprint. Discussion started: 6 August 2020

frequency of $PM_{2.5}$ pollution.

Many studies have indicated that $PM_{2.5}$ and O_3 pollution are strongly correlated with local meteorological factors such as temperature, relative humidity (RH) and WS (Huang et al., 2016; Miao et al., 2015; Shu et al., 2019; Tai et al., 2010). Miao et al. (2015) suggested that strong northwesterly synoptic winds, low BLH (boundary layer height), high RH and stable atmosphere are more prone to aerosol pollution in the BTH region during wintertime. Zhang et al. (2017) found that the majority of O_3 extremes occurred with daily maximum temperature (Tmax) between 300 K and 320 K, minimum RH (RHmin) less than 40%, and minimum WS less than 3 m s^{-1}, through the analysis of extreme O_3 and $PM_{2.5}$ events from historical data (30 years for O_3 and 10 years for $PM_{2.5}$) in the US. Furthermore, the number of annual extreme $PM_{2.5}$ days was highly positively correlated with the extreme RHmin/Tmax days, and the correlation coefficient between $PM_{2.5}$ and RHmin (Tmax) was highest in urban and suburban (rural) regions. Shi et al. (2020) studied the spatial distribution of O_3-8h (O_3 8-hour moving average) and $PM_{2.5}$, and their sensitivity of meteorological parameters; pronounced positive (negative) correlation between temperature (BLH and absolute humidity) and O_3-8h was found, but the relation between WS and O_3-8h was spatially different; for $PM_{2.5}$, it was negatively (positively) correlated with temperature, WS and BLH (absolute humidity). Recently, Han et al. (2020) revealed that meteorological factors can explain ~46% of the daily variability in summertime surface O_3, while synoptic factors contribute to ~37% of the overall meteorological effects on the daily variability of surface O_3 in eastern China. The abovementioned indicates that the variation of meteorological factors, which are mainly driven by the evolution of different weather circulation situations, play a non-negligible role in air pollution. Therefore, classification of air pollution according to the meteorological circulation has become particularly important, not least because of its worth when applied to air quality monitoring, forecasting and evaluation (Liu et al., 2019; Ning et al., 2019; Yang et al., 2018; Zheng et al., 2015).

In recent years, it has become possible to objectively classify atmospheric circulation conditions using weather data such as GH, sea level pressure, WS and temperature, so that the weather mechanism of extreme weather can be better understood and analyzed. Compared with subjective weather classification, the objective approach has been widely used in air pollution research (Beck & Philipp, 2010; Miao et al., 2017, 2019; Ning et al., 2018). Miao et al. (2019),

https://doi.org/10.5194/acp-2020-596
Preprint. Discussion started: 6 August 2020

based on the daily 900 hPa GH fields during winter in Beijing, identified seven synoptic patterns using an objective approach, and found that the weak northwesterly prevailing winds and strong elevated thermal inversion layer, along with the local emissions of aerosols play a decisive role in the formation of heavy pollution in Beijing; noted also that the southerly prevailing winds can transport the pollutants emitted from southern cities to Beijing. Zheng et al. (2015) studied the relationship between regional pollution and the patterns of large-scale atmospheric circulation over eastern China in October from 2001 to 2010 and identified six pollution types and three clean types. Specifically, weather patterns such as a uniform surface pressure field in eastern China or a steady straight westerly in the middle troposphere, particularly when at the rear of an anticyclone at 850 hPa, were found to be typically responsible for heavy pollution events. Many studies have suggested that $PM_{2.5}$ and O_3 pollution are mainly related to the East Asian summer monsoon (EASM) and western Pacific subtropical high (WPSH) (Li et al., 2018a; Xie et al., 2017; Yin et al., 2019; Zhao et al., 2010). The anomalous high-pressure system at 500 hPa, associated with downward dry, hot air and intense solar radiation can enhance the photochemical reactions to elevate the production of tropospheric O_3 (Gong and Liao, 2019; Yin et al., 2019). Furthermore, Zhao & Wang (2017) and Yin et al. (2019) noted that the positive GH anomalies at high latitudes tend to significantly weaken the cold-air advection from the north and result in local high temperatures near the surface in northern China, while the WPSH can transport sufficient water vapor to the YRD region and lead to a decrease in surface O_3. In addition, different subregions can exhibit various distributions of pollutant, even with identical emission scenarios (Li et al., 2019; Saikawa et al., 2017; C. Zhang et al., 2019). Also, it is still unclear how the distribution of pollution responds locally to large-scale atmospheric circulation patterns. Considering the reduced surface solar radiation due to $PM_{2.5}$ pollution (Haywood & Boucher, 2000; He & Wang, 2020; Huang et al., 2018; Yang et al., 2020) and thus suppressed the photochemical production of O_3 (Li et al., 2017), the compound O_3-$PM_{2.5}$ pollution-related meteorological conditions, should be complex and likely to be associated with certain weather types. Overall, the mechanism by which the synoptic weather pattern (SWP) modulates the characteristics of O_3-$PM_{2.5}$ compound pollution has yet to be comprehensively described.

In this study, the SWPs corresponding to the co-occurrence O_3-$PM_{2.5}$ pollution during

https://doi.org/10.5194/acp-2020-596
Preprint. Discussion started: 6 August 2020

summertime are analyzed, focusing on the eastern China (108°–135°E, 17°–53°N). Then, the causes of O_3-$PM_{2.5}$ compound pollution, as well as O_3-only pollution, from the perspective of the objective classification of atmospheric circulation patterns, are revealed. The findings are expected to provide a scientific reference for the monitoring, forecasting and evaluation of summertime air pollution in eastern China.

2. Data and methods

The air quality data, including $PM_{2.5}$, NO_2, O_3, and O_3-8h, are from the national 24-h continuous air quality observation published by the China Environmental Monitoring Station (http://www.cnemc.cn/). The hourly observation data of a total from 949 stations (108°–135°E, 17°–53°N) in eastern China during summertime of 2015–2018, which include the more prominent pollution areas in the eastern urban agglomeration, such as the BTH, YRD, PRD, Guanzhong Plain (GZP), Northeast Megalopolis (NEM) regions (the specific locations of stations and urban agglomerations are shown in Fig. 1a). Surface meteorological data, such as Tmax, precipitation, WS and RH from 517 meteorological observation stations and radiosonde data from 63 stations in eastern China, were obtained from the China National Meteorological Information Center of the China Meteorological Administration (http://data.cma.cn/site/index.html). The BLH was calculated according to the method given by Guo et al. (2016, 2019), and the FLWD [frequency of light wind (< 2 m s^{-1}) days], precipitation frequency (PF), and MDA8 O_3 were also counted.

Additionally, for synoptic analysis of particulate matter and O_3 pollution in summer, we use the GH field at 500 hPa and wind field at 850 hPa from the NCEP/NCAR (National Centers for Environmental Prediction/National Center for Atmospheric Research) daily reanalysis dataset on a 2.5° × 2.5° latitude/longitude grid during the study period.

The T-mode principal component analysis (T-PCA) is an objective mathematical computer-based method that can be used to classify the synoptic circulation patterns of regional gridded data in the troposphere at the lower level. Indeed, it is commonly regarded as the most promising weather pattern classification method at present (Huth et al., 2008). Moreover, this approach has been widely used in the studies of aerosols and O_3 pollution-related atmospheric circulation in China (Miao et al., 2017, 2019; Ning et al., 2018, 2019). The T-PCA analysis module of the COST733 software

https://doi.org/10.5194/acp-2020-596
Preprint. Discussion started: 6 August 2020

(http://cost733.met.no/) developed by the European Scientific and Technical Research Cooperation, was used to classify the synoptic circulation pattern based on the 500 hPa GH field. More detailed information about the T-PCA method can be found in Miao et al. (2017). To assess the performance of synoptic classification and determine the number of classes, the explained cluster variance (ECV) is selected in this study (Hoffmann & SchlüNzen, 2013; Ning et al., 2019; Philipp et al., 2014). The detailed information about the ECV is provided in the supplementary document.

Based on the GB3095-2012 environmental air quality standard issued by the Ministry of Ecology and Environment of China, O_3 ($PM_{2.5}$) pollution occurs when the MDA8 O_3 exceeds 160 (75) μg m^{-3}. To investigate the temporal variations of air pollution in various regions in summer, the pollution levels of O_3 and $PM_{2.5}$ in each key area were verified according to their concentration limits.

Finally, in order to make it clear in the analysis of different weather types of O_3 and $PM_{2.5}$ concentration change, we calculated the average distribution of O_3 and $PM_{2.5}$, as well as the meteorological conditions for each type, and further calculated the anomalous distribution of these variables, i.e., the average of O_3 and $PM_{2.5}$ and the average of the meteorological conditions under the respective patterns minus the average during summertime of 2015–2018, were given as well. The statistical significance was tested with a 0.05 confidence level via analysis of variance, which enabled us to distinguish the significant differences of spatial distribution characteristics between O_3 and $PM_{2.5}$ pollution under four SWPs.

3. Results

3.1 Spatial and temporal distribution of O_3 and $PM_{2.5}$ during summer 2015–2018

Figure 1 shows the summer averaged MDA8 O_3 and $PM_{2.5}$ concentrations at 949 stations in the eastern region of China for 2015–2018. Among these stations, the MDA8 O_3 concentration at most stations (662/949) exceeds 100 μg m^{-3}, of which 45 sites exceed 160 μg m^{-3}. The highest O_3 pollution is found in Zibo, Shandong, with a value of 181.5 μg m^{-3}. The averaged $PM_{2.5}$ at most sites (680/949) is below 35 μg m^{-3}, while reaches 62.6 μg m^{-3} in Handan, Hebei Province. On the whole, the MDA8 O_3 and $PM_{2.5}$ in the BTH region and its surrounding areas is significantly higher than in other regions; and besides, the level of O_3 in some urban clusters, such as the PRD, YRD,

https://doi.org/10.5194/acp-2020-596
Preprint. Discussion started: 6 August 2020

Atmospheric Chemistry and Physics
Discussions

GZP and NEM regions, is particularly higher than that of the surroundings, thus, we focus on analyzing these key areas later.

The temporal variations of O_3 pollution levels in key areas are displayed in Fig. 2, revealing an obvious increase in O_3 pollution levels and duration in the five priority areas for the period 2015–2018. The O_3 pollution in June is more severe than that in July and August, which is consistent with the fact that the peak concentration of MDA8 O_3 in northern China is in June (Gong and Liao, 2019). In spatial terms, O_3 pollution is particularly prominent in the BTH and GZP regions, with the number of pollution days reaching 148 and 109, of which even 23 and 17 are moderate pollution, respectively. Figure 3 illustrates the $PM_{2.5}$ pollution-level variations and, although it is not difficult to see that $PM_{2.5}$ pollution weakens year by year, the number of days of $PM_{2.5}$ pollution in the BTH region reaches 192 (25 days for moderate pollution), which is higher than the number of days of O_3 pollution. The reduced visibility of haze days weakens the solar radiation reaching the ground and inhibits photochemical reactions from generating O_3 (Li et al., 2019; Z. Zhang et al., 2015), as a result, the concentration of O_3 continues to increase with the mitigation of $PM_{2.5}$ pollution. It is worth noting that O_3 and $PM_{2.5}$ co-occurred in both the BTH (120 days) and GZP (60 days) regions. Overall, the O_3 and $PM_{2.5}$ concentration in eastern China exhibits distinct intraseasonal and interannual variations, indicating that, aside from the changes in emission sources (because it is considered that inter-seasonal and short-term changes in emission sources are not significant), it may also be regulated by meteorological conditions, which is further analyzed below.

3.2 Objective classification of large-scale synoptic circulation patterns in summer

To analyze the effect of meteorological conditions on the changes of O_3 and $PM_{2.5}$ concentration, it is necessary to statistically analyze the large-scale weather circulation situation in summer. Existing studies have shown that the WPSH (500 hPa GH field with obvious anticyclonic characteristics, and downward flow around the center) in summer prominently regulates the weather and climate of East Asia (Lu, 2002), owing to its various location, shape and intensity (Ding, 1994). A low-level southerly monsoon formed at the periphery of the WPSH can transport warm and humid air from the ocean to East Asia, which might also be responsible for the asymmetric spatial distribution in response to an enhanced WPSH for ground-level O_3, i.e. a decrease in southern China but an increase over northern China (Zhao & Wang, 2017).

Therefore, we used the T-PCA method to objectively classify the weather circulation of the 500-hPa GH field in the summers of 2015–2018, and finally obtained four SWPs related to the movement and development of the WPSH. The westward extension and southward motion of the WPSH in Type 1, as shown in Fig. 4a, transports water vapor into the YRD region, and the prevailing southwesterly in the YRD region and westward flow from the north form a cyclonic convergence area, with high temperature and high humidity during the Meiyu season. For Type 2, it is noticed that the westerly trough deepens accompanying the northward (or southward) advance (retreat) of WPSH, and the GH over northern China at 500 hPa is higher compared with Type 1 (Fig. 4b). The southerly wind blowing from the ocean to the continent lies in front of the bottom of the high pressure, affecting the southeastern region, while northern China is mainly controlled by the westerly trough, and the rain belt moves northwards to the east of the YRD region. Under Type 3, the WPSH shifts further north with a westward extension, and disintegrates a closed high-pressure monomer along the eastern coast of China, while the main body of the WPSH remains on the ocean (Fig. 4c). In this case, the YRD region is completely controlled by the monomer of the WPSH, which implies that the rainy season in the YRD region ends in midsummer and the weather becomes hot and dry. At the same time, the rain belt moves gradually northwards to the BTH and NEM regions. According to Fig. 4d, the monomer of WPSH under Type 4 continues to extend westwards and shift northwards, controlling northern China for a long time, and with persistent high temperatures and a heat wave occurring in most parts of the eastern China.

Fig. 5 presents the daily and annual variations of the SWPs in the summers of 2015–2018. The advance of the WPSH in eastern China occurs in June and July, while gradual withdrawal occurs mainly in August, so Type 1 mainly appears in June, while Type 2, Type 3 and Type 4 occurs mainly in July and August. Consequently, Type 1, Type 2, Type 3 and Type 4 appear for 167, 117, 52 and 32 days, respectively, during the study period. Since the movement of the WPSH is often affected by the activities of the surrounding weather system (such as typhoons, the Tibetan high, etc.) (Ge et al., 2019; Liu & You, 2020; Shu et al., 2016), there may be a short southward retreat during the WPSH's advancement (e.g., around 10 August 2018) and a short northward advance during its process of retreat (e.g., 21 and 29 August 2016). In general, it can be seen that the WPSH also shows

https://doi.org/10.5194/acp-2020-596
Preprint. Discussion started: 6 August 2020

evident intra-seasonal and interannual changes, which will inevitably regulate the weather, climate and environment changes in eastern China.

3.3 O_3 and $PM_{2.5}$ pollution characteristics under four SWPs

3.3.1 Spatial characteristics

We calculated the averaged and anomalous spatial distributions of the MDA8 of O_3 and $PM_{2.5}$ under the four SWPs. The averaged MDA8 O_3 under the four SWPs can be seen in Fig. S2. The O_3 concentration is relatively high in the area north of the Yangtze River under Type 1, and the high values of the MDA8 O_3 are mainly concentrated in the North China Plain (NCP) region, with a total of 94 stations surpassing 160 μg m^{-3}. Type 2 O_3 pollution is slightly weaker than that for Type 1, and the MDA8 O_3 at the 72 sites exceeds 160 μg m^{-3}. The O_3 high-value areas lie mainly in the NCP, GZP and YRD regions under Type 4, and there are 37 stations larger than 160 μg m^{-3}. Of the four SWPs, the lowest overall MDA8 O_3 occurs under Type 3, with only one site exceeding 160 μg m^{-3}. It is also found that the regions experiencing significant positive deviations of the MDA8 O_3 from the summer mean are as follows: the BTH, YRD and NEM regions under Type 1, the BTH and GZP regions under Type 2, the middle of the YRD and PRD regions under Type 3, and the YRD, GZP and PRD regions under Type 4 (Fig. 6).

Analogously, Fig. 7 shows the anomaly and significance of difference of $PM_{2.5}$ under the four weather types, presented as positive anomalies in the south of the BTH and YRD regions under Type 1, in the BTH, GZP and PRD regions under Type 2, and in the GZP and PRD regions under Type 4. Due to the obvious seasonal variations of $PM_{2.5}$ concentration (higher in winter and lower in summer) (H. Liu et al., 2019; Miao et al., 2015), no site exceeds 75 μg m^{-3} for the averaged $PM_{2.5}$ concentration. Even so, the level of $PM_{2.5}$ in the BTH region is still significantly higher under the four types than that for the other urban agglomerations (Fig. S3).

3.3.2 Pollution pattern differences in key areas

Air pollution in eastern China is principally found in dense urban areas such as the BTH and YRD regions (Gui et al., 2019; Han et al., 2019), so we took the BTH, PRD, YRD, GZP and NEM regions in the eastern region as key areas, counted the average daily changes of O_3 and $PM_{2.5}$ in

https://doi.org/10.5194/acp-2020-596
Preprint. Discussion started: 6 August 2020

Atmospheric Chemistry and Physics Discussions
Open Access
EGU

each key region under different weather patterns (Fig. 8), and calculated the over-limit ratio in key regions via the stations × days statistics (see Table 1). The diurnal variation of O_3 is more obvious, peaking at about 15:00 (Beijing time), while contrasting diurnal variations of $PM_{2.5}$ are given for different regions. According to Figure 8 and Table 1, the following characteristics can be identified for different urban clusters: (1) in the BTH region, the O_3 pollution of Type 1 and Type 2 is relatively serious, their over-standard rates reach 47.1% and 54.2%, and the $PM_{2.5}$ pollution rates of Type 2 and Type 1 reach 18.8% and 16.3%, respectively; (2) in the PRD region, the over-standard rates variation of O_3 and $PM_{2.5}$ is equable; (3) in the YRD region, the O_3 pollution over-limit ratio presents as Type 1 > Type 4 > Type 2 > Type 3, $PM_{2.5}$ pollution largely appears in Type1, and both O_3 and $PM_{2.5}$ in Type 1 are higher than those in the other types; (4) in the GZP region, the O_3 pollution frequency is higher in Type 2 and Type 4, and $PM_{2.5}$ pollution occurs more frequently in Type 2; and (5) in the NEM region, O_3 pollution is always found in Type 1, Type 2 and Type 4, but the over-standard rate is no more than 15% and $PM_{2.5}$ pollution in Type 1 is more than in Type 2.

In summary, Type 1 is prone to the formation of compound pollution of O_3-$PM_{2.5}$ (that is, when the ground MDA8 O_3 concentration exceeds 160 μg m^{-3}, the $PM_{2.5}$ concentration also exceeds 75 μg m^{-3}) in the southern BTH and northern YRD regions, which can be denoted as "South BTH – North YRD O_3-$PM_{2.5}$ compound pollution". Similarly, Type 2 can be denoted as "BTH – GZP O_3-$PM_{2.5}$ compound pollution", Type 3 as "BTH – GZP O_3-only pollution", and Type 4 as "GZP O_3-$PM_{2.5}$ compound pollution with BTH – YRD – PRD O_3-only pollution".

4. Discussion

4.1 Analysis of potential meteorological factors

The activities of atmospheric circulation system often lead to changes in meteorological elements, and to a large extent, affect the processes of pollutant formation, transmission and diffusion. Zhang et al. (2017) revealed that the extreme O_3 and $PM_{2.5}$ pollution events in the United States always occur under the conditions of high temperature, low humidity and low WS, while Miao et al. (2015) showed that RH is high when aerosol pollution occurs in the BTH region. However, O_3 pollution in China is more frequent in summer, and the warm and humid flow brought by the EASM makes summer always hot and moist. Zhao et al. (2019) investigated the RH of O_3

https://doi.org/10.5194/acp-2020-596
Preprint. Discussion started: 6 August 2020

pollution in Shijiazhuang between 15 June and 14 July 2016, and found that the O_3 concentration was higher at moderate humidity (RH average during daytime from 10:00 to 17:00 LT was 40%–50%).

Therefore, to explore the meteorological causes of O_3 and $PM_{2.5}$ pollution, we analyzed the distribution of the average and anomalies for Tmax, RH, PF, BLH and FLWD under the four SWPs (Figs. S4, S5, 9 and 10). Under the influence of the EASM, over 80% of the stations experience high temperatures (Tmax > 27°C) in each SWP, although the anomaly of Tmax in Type 1 presents negative. Type 1 is characterized by humid condition in the south and dry condition in the north, with the rain belt mainly in the PRD and YRD regions; Type 2 has dry and wet anomalies meridionally in northern China, and the rain band is located in the middle of the BTH and YRD regions; the RH is large for most sites under Type 3 and Type 4, corresponding to the shifted rain belt to the BTH and NEM regions under Type 3, and the heavy precipitation appeared in the western PRD region and the middle of the BTH and YRD regions under Type 4 (Fig. S4).

In terms of their anomalous spatial distribution, the positive anomalies of Tmax are located in the southern region of Type 3 and most of the eastern region of Type 4; and since Type 1 always appears in June, most areas are negative (Figs. 9a–d). For RH, Types 2, 3 and 4 are negative for the south and positive for the north, while Type 1 is opposite (Figs. 9e–h). PF is characterized by positive anomalies in the area south of the Yangtze River under Type 1, in the YRD region under Type 2, in the BTH and NEM regions under Type 3, and in the area between the BTH and YRD regions under Type 4 (Figs. 9i–l). As can be seen from Fig. 10, when the BLH has a positive anomaly, on the contrary FLWD has a negative anomaly, which indicates the higher the height of the boundary layer, the lower the frequency of light wind days, the more conducive to the diffusion of pollutants, and vice versa. After further inspection of Fig. S4, we found the YRD region in Type 1, the area north of the Yangtze River in Type 2, the BTH and PRD regions in Type 3, and most regions of Type 4 have shallow BLHs and high FLWDs, which is detrimental to the transportation of pollution in these areas, thus corresponding to high levels of pollution under these weather patterns.

4.2 Effects of NO_2 on O_3

Photochemical production of O_3 mainly involve emissions of VOCs and NO_x from anthropogenic, biogenic and biomass burning sources (Deng et al., 2019; Gvozdić et al., 2011;

https://doi.org/10.5194/acp-2020-596
Preprint. Discussion started: 6 August 2020

Sillman, 2002). Due to the implementation of a number of pollution abatement measures, the abundance of NO_2 has decreased significantly in eastern China in the past few years, leading to the sensitive precursor of O_3 formation changing from VOCs to a mixture of VOCs and NO_x (Wang et al., 2019b). As a result, both NO_x and VOCs need being cooperatively controlled to mitigate O_3 pollution. Figure 11 shows the diurnal variations of NO_2 and the ratio of O_3 to NO_2 (O_3/NO_2) in five urban clusters, where the larger the O_3/NO_2 ratio, the more O_3 is generated by the photochemical reaction of NO_2. The NO_2 concentration reaches its lowest and O_3/NO_2 reaches a peak at around 15:00 (Beijing time) in the day, owing to the rapid consumption of NO_2 by the photochemical reaction under high temperature and strong solar radiation in the afternoon. As far as O_3/NO_2 (NO_2) is concerned, it can be seen that the daytime O_3/NO_2 (NO_2) values under Type 4 in the five regions is greater than (less than) under the other types, indicating that O_3 photochemical reactions are stronger under this type than the others. In contrast, the photochemical reaction of the BTH and NEM regions under Type 3 and the YRD region under Type 1 is weaker owing to the warm and humid air brought by the WPSH, and the rainy weather is also unconducive to the occurrence of photochemical reactions to generate O_3. For the PRD region, the photochemical processes of the four SWPs are not significantly different. It can be seen that different weather patterns also have an important regulatory effect on the photochemical production of O_3.

In summary, the different SWPs can modulate the regional variability of summertime O_3 and $PM_{2.5}$ and their causes in summer as follows:

(1) Type 1: The area to the north of the Yangtze River under Type 1 is controlled by the westerly zone in the north of the WPSH at 500 hPa. Under the conditions of high temperature (Tmax > 27°C), moderate humidity (RH ~60%), and low PF, photochemical reactions are largely promoted to cause severe O_3 pollution. Meanwhile, the area from south of the BTH region to north of the YRD region is located in front of the westerly trough, under the influence of the warm and humid air of the WPSH, and so the hygroscopic growth of fine particulates will cause a certain amount of $PM_{2.5}$ pollution, becoming O_3-$PM_{2.5}$ compound pollution (Fig. 12). In Figure S6, we counted the number and probability of occurrence of compound pollution days in each site in summer during 2015-2018, indicating that high occurrence probability (maximum values can approach 46.7%) of compound pollution appeared in the Northern China plain (to the north of 32°N). About 55.6% of compound

https://doi.org/10.5194/acp-2020-596
Preprint. Discussion started: 6 August 2020

pollution occurrence days at all sites occurred under Type 1.

(2) Type 2: The westerly trough strengthens meridionally, and the northern region is still controlled by the westerly zone. Ozone pollution is severe under the meteorological conditions of high temperature, moderate humidity, and few precipitations. The $PM_{2.5}$ in the BTH region, which is located in front of the westerly trough, is high since the shallow boundary layer and low wind frequency are unfavorable for pollutant diffusion. Therefore, O_3-$PM_{2.5}$ compound pollution can also be rather frequent (Fig. 12). About 33.0% of compound pollution occurrence days at all sites occurred under Type 2 in summer during 2015-2018.

(3) Type 3: High temperature, low humidity and few precipitations in the YRD region generates a large amount of O_3, while the positive BLH and negative FLWD anomalies are unfavorable to O_3 accumulation. On the other hand, summer typhoon activities will weaken the WPSH intensity over the YRD region, leading to the eastward retreat and northward shift of the WPSH, high WS in coastal areas that will ease O_3 pollution on the ground (Shu et al., 2016), and high PF in the BTH and PRD regions which tend to suppress O_3 production. Accordingly, Type 3 is characterized as light O_3-only pollution in the areas of the BTH, YRD and PRD (Fig. 12).

(4) Type 4: High temperatures, medium-high humidity and few precipitations in the GZP and PRD regions can cause O_3-$PM_{2.5}$ compound pollution, but $PM_{2.5}$ pollution in the PRD region is not heavy, which is possibly in relation to local lower pollutant emissions. Under the control of the WPSH, there are strong photochemical reactions at high temperatures and little rainfall in the BTH region, which is also conducive to O_3 generation (Fig. 12). Meanwhile, relative to Type 1, O_3 pollution is lighter in the BTH, due to the differences of RH, BLH and FLWD.

5 Conclusions

In this study, T-PCA, an objective classification method, was applied to classify the 500-hPa weather circulation pattern as four SWPs in the summers of 2015–2018. It was found that these four SWPs are closely related to the development of the WPSH. The spatial and temporal distribution characteristics of O_3 and $PM_{2.5}$ pollution in eastern China under the four SWPs were analyzed to regulate and differentiate O_3 and $PM_{2.5}$ pollution in key areas. We find two synoptic patterns are prone to lead to co-occurrence of O_3 and $PM_{2.5}$ pollution: in the southern BTH and northern YRD regions under Type 1 and the areas in the BTH and GZP under Type 2 are associated with the double

https://doi.org/10.5194/acp-2020-596
Preprint. Discussion started: 6 August 2020

high level of O_3 and $PM_{2.5}$. About 55.6% of compound pollution occurrence days at all sites occurred under Type 1 while 33.0% under Type 2.

Type 1 weather pattern appears frequently in June, with a stable WPSH ridge line at about 22°N, and the warm and humid air brought by the WPSH reaches the area south of the Yangtze River, where a high temperature and high humidity Meiyu season is formed which suppresses the photochemical reaction of O_3 generation. Meanwhile, the north of China is controlled by a low-pressure trough with high temperatures and little rain. The hygroscopic growth of $PM_{2.5}$ occurs in the corresponding area in front of the trough with a small amount of water vapor transported by the WPSH, causing compound pollution of O_3 and $PM_{2.5}$ in the south of the BTH region and north of the YRD region; particularly, unfavorable pollution diffusion conditions of a shallow BLH and low WS further exacerbate the severity of this compound pollution.

Under Type 2, the WPSH shifts northwards and retreats eastwards (sometimes retreats southwards and eastwards), with the meridional deepening of the East Asian major trough, and thus warm and humid airstreams are brought to the Northern China (e.g., the BTH region), gradually elevating temperatures and humidity. Although positive RH anomaly promotes hygroscopic growth of the $PM_{2.5}$, water vapor leads a sink of ozone by contrast. As a result, the probability of double high level of O_3 and $PM_{2.5}$ under Type 2 is less than Type 1, the extent of compound pollution in Type 2 is also narrowed. On the other hand, weak precipitation, shallow boundary layer and low wind speed tend to create favorable conditions for pollution maintenance.

In general, the location of the WPSH is tightly associated with O_3 pollution in eastern China, and the changes of meteorological conditions in different regions affected by the WPSH can induce significant regional differences in O_3 and $PM_{2.5}$ pollution. More importantly, the effects of various large-scale weather circulation patterns on the O_3-$PM_{2.5}$ compound pollution and their corresponding physical and chemical processes, have been clarified, which has important scientific reference value in summer air-quality forecasts, as well as assessment and policy-making services.

Data availability

Hourly $PM_{2.5}$, NO_2, O_3, and O_3-8h data is published by the China Environmental Monitoring Station (http://www.cnemc.cn/). Surface meteorological data, such as Tmax, precipitation, WS and RH, radiosonde data can be obtained from the China National Meteorological Information Center of the China Meteorological Administration (http://data.cma.cn/site/index.html). The NCEP/NCAR daily reanalysis dataset can be download from https://psl.noaa.gov/data/gridded/data.ncep.reanalysis.html.

Author contributions

L. Zong: Methodology, Data Curation, Formal Analysis, Writing- Original draft preparation, Results Discussion, Writing- Reviewing and Editing；Y. Yang: Conceptualization, Methodology, Formal Analysis, Results Discussion, Writing- Reviewing and Editing；M. Gao, H. Wang, P. Wang, L. Wang, H. Zhang, G. Ning, C. Liu, Y. Li, Z. Gao: Results Discussion, Comments, Writing- Reviewing and Editing

Competing interests

The authors declare that they have no conflict of interests

Acknowledgments

This study was jointly funded by supported by the National Key Research and Development Program of China (2018YFC1506502) and the National Natural Science Foundation of China (41871029).

References

Amil, N., Latif, M. T., Khan, M. F. and Mohamad, M.: Seasonal variability of PM2.5composition and sources in the Klang Valley urban-industrial environment, Atmos. Chem. Phys., 16(8), 5357–5381, doi:10.5194/acp-16-5357-2016, 2016.

Beck, C. and Philipp, A.: Evaluation and comparison of circulation type classifications for the European domain, Phys. Chem. Earth, 35(9–12), 374–387, doi:10.1016/j.pce.2010.01.001, 2010.

Cai, W., Li, K., Liao, H., Wang, H. and Wu, L.: Weather conditions conducive to Beijing severe haze more frequent under climate change, Nat. Clim. Chang., 7(4), 257–262, doi:10.1038/nclimate3249, 2017.

Chen, C., Saikawa, E., Comer, B., Mao, X. and Rutherford, D.: Ship Emission Impacts on Air Quality and Human Health in the Pearl River Delta (PRD) Region, China, in 2015, With Projections to 2030, GeoHealth, 3(9), 284–306, doi:10.1029/2019GH000183, 2019.

Cohen, A. J., Brauer, M., Burnett, R., Anderson, H. R., Frostad, J., Estep, K., Balakrishnan, K., Brunekreef, B., Dandona, L., Dandona, R., Feigin, V., Freedman, G., Hubbell, B., Jobling, A., Kan, H., Knibbs, L., Liu, Y., Martin, R., Morawska, L., Pope, C. A., Shin, H., Straif, K., Shaddick, G., Thomas, M., van Dingenen, R., van Donkelaar, A., Vos, T., Murray, C. J. L. and Forouzanfar, M. H.: Estimates and 25-year trends of the global burden of disease attributable to ambient air pollution: an analysis of data from the Global Burden of Diseases Study 2015, Lancet, 389(10082), 1907–1918, doi:10.1016/S0140-6736(17)30505-6, 2017.

Day, D. B., Xiang, J., Mo, J., Li, F., Chung, M., Gong, J., Weschler, C. J., Ohman-Strickland, P. A., Sundell, J., Weng, W., Zhang, Y. and Zhang, J. J.: Association of ozone exposure with cardiorespiratory pathophysiologic mechanisms in healthy adults, JAMA Intern. Med., 177(9), 1344–1353, doi:10.1001/jamainternmed.2017.2842, 2017.

Deng, Y., Li, J., Li, Y., Wu, R. and Xie, S.: Characteristics of volatile organic compounds, NO2, and effects on ozone formation at a site with high ozone level in Chengdu, J. Environ. Sci. (China), 75(2), 334–345, doi:10.1016/j.jes.2018.05.004, 2019.

Ding, Y.: The Summer Monsoon in East Asia, in Monsoons over China, pp. 1–90., 1994.

Du, Y., Wan, Q., Liu, H., Liu, H., Kapsar, K. and Peng, J.: How does urbanization influence PM 2.5 concentrations? Perspective of spillover effect of multi-dimensional urbanization impact, J. Clean. Prod., 220, 974–983, doi:10.1016/j.jclepro.2019.02.222, 2019.

Fan, H., Zhao, C. and Yang, Y.: A comprehensive analysis of the spatio-temporal variation of urban air pollution in China during 2014–2018, Atmos. Environ., 220(November), 117066, doi:10.1016/j.atmosenv.2019.117066, 2020.

Ge, J., You, Q. and Zhang, Y.: Effect of Tibetan Plateau heating on summer extreme precipitation in eastern China, Atmos. Res., 218, 364–371, doi:10.1016/j.atmosres.2018.12.018, 2019.

Gong, C. and Liao, H.: A typical weather pattern for ozone pollution events in North China, Atmos. Chem. Phys., 19(22), 13725–13740, doi:10.5194/acp-19-13725-2019, 2019.

Gu, Y., Wong, T. W., Law, S., Dong, G., Ho, K. F., Yang, Y. and Yim, S. H. L.: Impacts of sectoral emissions in China and the implications: Air quality, public health, crop production, and economic costs, Environ. Res. Lett., 13, doi:10.1088/1748-9326/aad138, 2018.

Gui, K., Che, H., Wang, Y., Wang, H., Zhang, L., Zhao, H., Zheng, Y., Sun, T. and Zhang, X.: Satellite-derived PM2.5 concentration trends over Eastern China from 1998 to 2016: Relationships to emissions and meteorological parameters, Environ. Pollut., 247, 1125–1133, doi:10.1016/j.envpol.2019.01.056, 2019.

Guo, J., Miao, Y., Zhang, Y., Liu, H., Li, Z., Zhang, W., He, J., Lou, M., Yan, Y., Bian, L. and Zhai, P.: The climatology of planetary boundary layer height in China derived from radiosonde and reanalysis data, Atmos. Chem. Phys., 16(20), 13309–13319, doi:10.5194/acp-16-13309-2016, 2016.

Guo, J., Li, Y., Cohen, J. B., Li, J., Chen, D., Xu, H., Liu, L., Yin, J., Hu, K. and Zhai, P.: Shift in the Temporal Trend of Boundary Layer Height in China Using Long-Term (1979–2016) Radiosonde Data, Geophys. Res. Lett., 46(11), 6080–6089, doi:10.1029/2019GL082666, 2019.

Gvozdić, V., Kovač-Andrić, E. and Brana, J.: Influence of Meteorological Factors NO2, SO2, CO and PM10 on the Concentration of O3 in the Urban Atmosphere of Eastern Croatia, Environ. Model. Assess., 16(5), 491–501, doi:10.1007/s10666-011-9256-4, 2011.

Han, H., Liu, J., Shu, L., Wang, T. and Yuan, H.: Local and synoptic meteorological influences on daily variability of summertime surface ozone in eastern China, Atmos. Chem. Phys. Discuss., (July), 1–51, doi:10.5194/acp-2019-494, 2019.

Han, H., Liu, J., Shu, L., Wang, T. and Yuan, H.: Local and synoptic meteorological influences on daily variability in summertime surface ozone in eastern China, Atmos. Chem. Phys., 20(1), 203–222, doi:10.5194/acp-20-203-2020, 2020.

Haywood, J. and Boucher, O.: Estimates of the direct and indirect radiative forcing due to tropospheric aerosols: A review, Rev. Geophys., 38(4), 513–543, doi:10.1029/1999RG000078, 2000.

He, Y. and Wang, K.: Variability in Direct and Diffuse Solar Radiation Across China From 1958 to 2017, Geophys. Res. Lett., 47(1), doi:10.1029/2019GL084570, 2020.

Hoffmann, P. and Heinke SchlüNzen, K.: Weather pattern classification to represent the urban heat island in present and future climate, J. Appl. Meteorol. Climatol., 52(12), 2699–2714, doi:10.1175/JAMC-D-12-065.1, 2013.

Huang, X., Ding, A., Liu, L., Liu, Q., Ding, K., Nie, W., Xu, Z., Chi, X., Wang, M., Sun, J., Guo, W. and Fu, C.: Effects of aerosol-radiation interaction on precipitation during biomass-burning season in East China, Atmos. Chem. Phys. Discuss., (April), 1–37, doi:10.5194/acp-2016-272, 2016.

Huang, X., Wang, Z. and Ding, A.: Impact of Aerosol-PBL Interaction on Haze Pollution: Multiyear Observational Evidences in North China, Geophys. Res. Lett., 45(16), 8596–8603, doi:10.1029/2018GL079239, 2018.

Huth, R., Beck, C., Philipp, A., Demuzere, M., Ustrnul, Z., Cahynová, M., Kyselý, J. and Tveito, O. E.: Classifications of atmospheric circulation patterns: Recent advances and applications, Ann. N. Y. Acad. Sci., 1146, 105–152, doi:10.1196/annals.1446.019, 2008.

Ji, X., Yao, Y. and Long, X.: What causes PM2.5 pollution? Cross-economy empirical analysis from socioeconomic perspective, Energy Policy, 119(April), 458–472, doi:10.1016/j.enpol.2018.04.040, 2018.

Li, K., Jacob, D. J., Liao, H., Zhu, J., Shah, V., Shen, L., Bates, K. H., Zhang, Q. and Zhai, S.: A two-pollutant strategy for improving ozone and particulate air quality in China, Nat. Geosci., 12(11), 906–910, doi:10.1038/s41561-019-0464-x, 2019.

Li, M., Wang, T., Xie, M., Zhuang, B., Li, S., Han, Y., Song, Y. and Cheng, N.: Improved meteorology and ozone air quality simulations using MODIS land surface parameters in the Yangtze River Delta urban cluster, China, J. Geophys. Res., 122(5), 3116–3140, doi:10.1002/2016JD026182, 2017a.

Li, M., Wang, T., Han, Y., Xie, M., Li, S., Zhuang, B. and Chen, P.: Modeling of a severe dust event and its impacts on ozone photochemistry over the downstream Nanjing megacity of eastern China, Atmos. Environ., 160, 107–123, doi:10.1016/j.atmosenv.2017.04.010, 2017b.

Li, M., Wang, L., Liu, J., Gao, W., Song, T., Sun, Y., Li, L., Li, X., Wang, Y., Liu, L., Daellenbach, K. R., Paasonen, P. J., Kerminen, V. M., Kulmala, M. and Wang, Y.: Exploring the regional pollution characteristics and meteorological formation mechanism of PM2.5 in North China during 2013–2017, Environ. Int., 134(November 2019), 105283, doi:10.1016/j.envint.2019.105283, 2020.

Li, S., Wang, T., Huang, X., Pu, X., Li, M., Chen, P., Yang, X. Q. and Wang, M.: Impact of East Asian Summer Monsoon on Surface Ozone Pattern in China, J. Geophys. Res. Atmos., 123(2), 1401–1411, doi:10.1002/2017JD027190, 2018a.

Li, Z., Guo, J., Ding, A., Liao, H., Liu, J., Wang, T., Xue, H., Zhang, H. and Zhu, B.: Special Topic ： Atmosphere Pollution and Control Review ENVIRONMENT / ECOLOGY Aerosol and Boundary-Layer Interactions and Impact on Air Quality, , (January), doi:10.1093/nsr/nwx117/4191281, 2018b.

Liu, H., Tian, H., Zhang, K., Liu, S., Cheng, K., Yin, S., Liu, Y., Liu, X., Wu, Y., Liu, W., Bai, X., Wang, Y., Shao, P., Luo, L., Lin, S., Chen, J. and Liu, X.: Seasonal variation, formation mechanisms and potential sources of PM2.5 in two typical cities in the Central Plains Urban Agglomeration, China, Sci. Total Environ., 657, 657–670, doi:10.1016/j.scitotenv.2018.12.068, 2019a.

Liu, J. and You, Q.: A diagnosis of the interannual variation of the summer hydrometeor based on ERA-interim over Eastern China, Atmos. Res., 231(October 2018), 104654, doi:10.1016/j.atmosres.2019.104654, 2020.

Liu, N., Zhou, S., Liu, C. and Guo, J.: Synoptic circulation pattern and boundary layer structure associated with PM2.5 during wintertime haze pollution episodes in Shanghai, Atmos. Res., 228(46), 186–195, doi:10.1016/j.atmosres.2019.06.001, 2019b.

Ma, Z., Hu, X., Sayer, A. M., Levy, R., Zhang, Q., Xue, Y., Tong, S., Bi, J., Huang, L. and Liu, Y.: Satellite-based spatiotemporal trends in PM2.5 concentrations: China, 2004-2013, Environ. Health Perspect., 124(2), 184–192, doi:10.1289/ehp.1409481, 2016.

Miao, Y., Hu, X.-M., Liu, S., Qian, T., Xue, M., Zheng, Y. and Wang, S.: Seasonal variation of local atmospheric circulations and boundary layer structure in the Beijing-Tianjin-Hebei region and implications for air quality., J. Adv. Model. Earth Syst., 7, 1602–1626, doi:10.1002/2015ms000522, 2015.

Miao, Y., Guo, J., Liu, S., Liu, H., Li, Z., Zhang, W. and Zhai, P.: Classification of summertime synoptic patterns in Beijing and their associations with boundary layer structure affecting aerosol pollution, Atmos. Chem. Phys., 17(4), 3097–3110, doi:10.5194/acp-17-3097-2017, 2017.

Miao, Y., Liu, S. and Huang, S.: Synoptic pattern and planetary boundary layer structure associated with aerosol pollution during winter in Beijing, China, Sci. Total Environ., 682, 464–474, doi:10.1016/j.scitotenv.2019.05.199, 2019.

Ning, G., Wang, S., Yim, S. H. L., Li, J., Hu, Y., Shang, Z., Wang, J. and Wang, J.: Impact of low-pressure systems on winter heavy air pollution in the northwest Sichuan Basin, China, Atmos. Chem. Phys., 18(18), 13601–13615, doi:10.5194/acp-18-13601-2018, 2018.

Ning, G., Yim, S. H. L., Wang, S., Duan, B., Nie, C., Yang, X., Wang, J. and Shang, K.: Synergistic effects of synoptic weather patterns and topography on air quality: a case of the Sichuan Basin of China, Clim. Dyn., 53(11), 6729–6744, doi:10.1007/s00382-019-04954-3, 2019.

Philipp, A., Beck, C., Esteban, P., Krennert, T., Lochbihler, K., Spyros, P., Pianko-kluczynska, K., Post, P., Alvarez, R., Spekat, A. and Streicher, F.: Cost733 user guide., 2014.

Riyu, L.: Indices of the Summertime Western North Pacific Subtropical High, Adv. Atmos. Sci., 19(6), 1004–1028, doi:10.1007/s00376-002-0061-5, 2002.

Saikawa, E., Kim, H., Zhong, M., Avramov, A., Zhao, Y., Janssens-Maenhout, G., Kurokawa, J. I., Klimont, Z., Wagner, F., Naik, V., Horowitz, L. W. and Zhang, Q.: Comparison of emissions inventories of anthropogenic air pollutants and greenhouse gases in China, Atmos. Chem. Phys., 17(10), 6393–6421, doi:10.5194/acp-17-6393-2017, 2017.

Shi, Z., Huang, L., Li, J., Ying, Q., Zhang, H. and Hu, J.: Sensitivity Analysis of the Surface Ozone and Fine Particulate Matter to Meteorological Parameters in China, Atmos. Chem. Phys. Discuss., 2020, 1–29, doi:10.5194/acp-2020-173, 2020.

Shu, L., Xie, M., Wang, T., Gao, D., Chen, P., Han, Y., Li, S., Zhuang, B. and Li, M.: Integrated studies of a regional ozone pollution synthetically affected by subtropical high and typhoon system in the Yangtze River Delta region, China, Atmos. Chem. Phys., 16(24), 15801–15819, doi:10.5194/acp-16-15801-2016, 2016.

Shu, L., Wang, T., Xie, M., Li, M., Zhao, M., Zhang, M. and Zhao, X.: Episode study of fine particle and ozone during the CAPUM-YRD over Yangtze River Delta of China: Characteristics and source attribution, Atmos. Environ., 203(July 2018), 87–101, doi:10.1016/j.atmosenv.2019.01.044, 2019.

Sillman, S.: Chapter 12 The relation between ozone, NOx and hydrocarbons in urban and polluted rural environments, Dev. Environ. Sci., 1(C), 339–385, doi:10.1016/S1474-8177(02)80015-8, 2002.

Song, C., Wu, L., Xie, Y., He, J., Chen, X., Wang, T., Lin, Y., Jin, T., Wang, A., Liu, Y., Dai, Q., Liu, B., Wang, Y. nan and Mao, H.: Air pollution in China: Status and spatiotemporal variations, Environ. Pollut., 227, 334–347, doi:10.1016/j.envpol.2017.04.075, 2017.

Sun, L., Xue, L., Wang, T., Gao, J., Ding, A., Cooper, O. R., Lin, M., Xu, P., Wang, Z., Wang, X., Wen, L., Zhu, Y., Chen, T., Yang, L., Wang, Y., Chen, J. and Wang, W.: Significant increase of summertime ozone at Mount Tai in Central Eastern China, Atmos. Chem. Phys., 16(16), 10637–10650, doi:10.5194/acp-16-10637-2016, 2016.

Tai, A. P. K., Mickley, L. J. and Jacob, D. J.: Correlations between fine particulate matter (PM2.5) and meteorological variables in the United States: Implications for the sensitivity of PM2.5 to climate change, Atmos. Environ., 44(32), 3976–3984, doi:10.1016/j.atmosenv.2010.06.060, 2010.

Wang, H., Li, J., Gao, Z., Yim, S. H. L., Shen, H., Ho, H. C., Li, Z., Zeng, Z., Liu, C., Li, Y., Ning, G. and Yang, Y.: High-spatial-resolution population exposure to PM2.5 pollution based on multi-satellite retrievals: A case study of seasonal variation in the Yangtze River Delta, China in 2013, Remote Sens., 11(23), doi:10.3390/rs11232724, 2019a.

Wang, H. J. and Chen, H. P.: Understanding the Recent Trend of Haze Pollution in Eastern China: Roles of Climate Change, Atmos. Chem. Phys. Discuss., 2016(January), 1–18, doi:10.5194/acp-2015-1009, 2016.

Wang, N., Lyu, X., Deng, X., Huang, X., Jiang, F. and Ding, A.: Aggravating O 3 pollution due to NO x emission control in eastern China, Sci. Total Environ., 677(x), 732–744, doi:10.1016/j.scitotenv.2019.04.388, 2019b.

Xie, M., Shu, L., Wang, T., Gao, D., Li, S., Zhuang, B., Huang, A., Fang, D., Han, Y., Li, M., Chen, P., Liu, Z., Wu, Z. and Lu, H.: Inter-annual variation of aerosol pollution in East Asia and its relation with strong/weak East Asian winter monsoon, Atmos. Chem. Phys. Discuss., (June), 1–38, doi:10.5194/acp-2017-500, 2017.

Yang, Y., Zheng, X., Gao, Z., Wang, H., Wang, T., Li, Y., Lau, G. N. C. and Yim, S. H. L.: Long-Term Trends of Persistent Synoptic Circulation Events in Planetary Boundary Layer and Their Relationships With Haze Pollution in Winter Half Year Over Eastern China, J. Geophys. Res. Atmos., 123(19), 10,991-11,007, doi:10.1029/2018JD028982, 2018.

Yang, Y., Zheng, Z., Yim, S. Y. L., Roth, M., Ren, G., Gao, Z., Wang, T., Li, Q., Shi, C., Ning, G. and Li, Y.: PM2.5 Pollution Modulates Wintertime Urban Heat Island Intensity in the Beijing-Tianjin-Hebei Megalopolis, China, Geophys. Res. Lett., 47(1), 0–3, doi:10.1029/2019GL084288, 2020.

Ye, W. F., Ma, Z. Y. and Ha, X. Z.: Spatial-temporal patterns of PM2.5 concentrations for 338 Chinese cities, Sci. Total Environ., 631–632, 524–533, doi:10.1016/j.scitotenv.2018.03.057, 2018.

Yim, S. H. L., Wang, M., Gu, Y., Yang, Y., Dong, G. and Li, Q.: Effect of Urbanization on Ozone and Resultant Health Effects in the Pearl River Delta Region of China, J. Geophys. Res. Atmos., 124(21), 11568–11579, doi:10.1029/2019JD030562, 2019.

Yin, Z., Cao, B. and Wang, H.: Dominant patterns of summer ozone pollution in eastern China and associated atmospheric circulations, Atmos. Chem. Phys., 19(22), 13933–13943, doi:10.5194/acp-19-13933-2019, 2019.

Yue, X., Unger, N., Harper, K., Xia, X., Liao, H., Zhu, T., Xiao, J., Feng, Z. and Li, J.: Ozone and haze pollution weakens net primary productivity in China, Atmos. Chem. Phys., 17(9), 6073–6089, doi:10.5194/acp-17-6073-2017, 2017.

Zhang, C., Liu, C., Hu, Q., Cai, Z., Su, W., Xia, C., Zhu, Y., Wang, S. and Liu, J.: Satellite UV-Vis spectroscopy: implications for air quality trends and their driving forces in China during 2005–

https://doi.org/10.5194/acp-2020-596
Preprint. Discussion started: 6 August 2020

Atmospheric Chemistry and Physics
Open Access
Discussions

2017, Light Sci. Appl., 8(1), doi:10.1038/s41377-019-0210-6, 2019a.

Zhang, H., Wang, Y., Park, T. W. and Deng, Y.: Quantifying the relationship between extreme air pollution events and extreme weather events, Atmos. Res., 188, 64–79, doi:10.1016/j.atmosres.2016.11.010, 2017.

Zhang, Q., Zheng, Y., Tong, D., Shao, M., Wang, S., Zhang, Y., Xu, X., Wang, J., He, H., Liu, W., Ding, Y., Lei, Y., Li, J., Wang, Z., Zhang, X., Wang, Y., Cheng, J., Liu, Y., Shi, Q., Yan, L., Geng, G., Hong, C., Li, M., Liu, F., Zheng, B., Cao, J., Ding, A., Gao, J., Fu, Q., Huo, J., Liu, B., Liu, Z., Yang, F., He, K. and Hao, J.: Drivers of improved PM2.5 air quality in China from 2013 to 2017, Proc. Natl. Acad. Sci. U. S. A., 116(49), 24463–24469, doi:10.1073/pnas.1907956116, 2019b.

Zhang, R. H., Li, Q. and Zhang, R. N.: Meteorological conditions for the persistent severe fog and haze event over eastern China in January 2013, Sci. China Earth Sci., 57(1), 26–35, doi:10.1007/s11430-013-4774-3, 2014.

Zhang, W., Wang, H., Zhang, X., Peng, Y., Zhong, J., Wang, Y. and Zhao, Y.: Evaluating the contributions of changed meteorological conditions and emission to substantial reductions of PM2.5 concentration from winter 2016 to 2017 in Central and Eastern China, Sci. Total Environ., 716, 136892, doi:10.1016/j.scitotenv.2020.136892, 2020.

Zhang, Y., Ding, A., Mao, H., Nie, W., Zhou, D., Liu, L., Huang, X. and Fu, C.: Impact of synoptic weather patterns and inter-decadal climate variability on air quality in the North China Plain during 1980-2013, Atmos. Environ., 124, 119–128, doi:10.1016/j.atmosenv.2015.05.063, 2016a.

Zhang, Y. L. and Cao, F.: Fine particulate matter (PM 2.5) in China at a city level, Sci. Rep., 5(2014), 1–12, doi:10.1038/srep14884, 2015.

Zhang, Z., Zhang, X., Gong, D., Quan, W., Zhao, X., Ma, Z. and Kim, S. J.: Evolution of surface O3 and PM2.5 concentrations and their relationships with meteorological conditions over the last decade in Beijing, Atmos. Environ., 108, 67–75, doi:10.1016/j.atmosenv.2015.02.071, 2015.

Zhang, Z., Zhang, X., Gong, D., Kim, S. J., Mao, R. and Zhao, X.: Possible influence of atmospheric circulations on winter haze pollution in the Beijing-Tianjin-Hebei region, northern China, Atmos. Chem. Phys., 16(2), 561–571, doi:10.5194/acp-16-561-2016, 2016b.

Zhao, C., Wang, Y., Yang, Q., Fu, R., Cunnold, D. and Choi, Y.: Impact of East Asian summer monsoon on the air quality over China: View from space, J. Geophys. Res. Atmos., 115(9), 1–12, doi:10.1029/2009JD012745, 2010.

https://doi.org/10.5194/acp-2020-596
Preprint. Discussion started: 6 August 2020

Zhao, W., Tang, G., Yu, H., Yang, Y., Wang, Y., Wang, L., An, J., Gao, W., Hu, B., Cheng, M., An, X., Li, X. and Wang, Y.: Evolution of boundary layer ozone in Shijiazhuang, a suburban site on the North China Plain, J. Environ. Sci. (China), 83, 152–160, doi:10.1016/j.jes.2019.02.016, 2019.

Zhao, Z. and Wang, Y.: Influence of the West Pacific subtropical high on surface ozone daily variability in summertime over eastern China, Atmos. Environ., 170, 197–204, doi:10.1016/j.atmosenv.2017.09.024, 2017.

Zheng, X. Y., Fu, Y. F., Yang, Y. J. and Liu, G. S.: Impact of atmospheric circulations on aerosol distributions in autumn over eastern China: Observational evidence, Atmos. Chem. Phys., 15(21), 12115–12138, doi:10.5194/acp-15-12115-2015, 2015.

Zhong, M., Chen, F. and Saikawa, E.: Sensitivity of projected PM2.5- and O3-related health impacts to model inputs: A case study in mainland China, Environ. Int., 123(May 2018), 256–264, doi:10.1016/j.envint.2018.12.002, 2019.

Zhu, J., Liao, H. and Li, J.: Increases in aerosol concentrations over eastern China due to the decadal-scale weakening of the East Asian summer monsoon, Geophys. Res. Lett., 39(9), 1–6, doi:10.1029/2012GL051428, 2012.

https://doi.org/10.5194/acp-2020-596
Preprint. Discussion started: 6 August 2020

Table 1. Over-limit ratio and concentration of MDA8 O_3 and PM2.5 calculated via stations × days in key urban clusters under four SWPs

Urban cluster	Month	Type1					Type2					Type3					Type4				
		Stas × days	MDA O_3		$PM_{2.5}$		Stas × days	MDA O_3		$PM_{2.5}$		Stas × days	MDA O_3		$PM_{2.5}$		Stas × days	MDAO_3		$PM_{2.5}$	
			OLR	Con	OLR	Con		OLR	Con	OLR	Con		OLR	Con	OLR	Con		OLR	Con	OLR	Con
BTH	6	6416	57.3%	172.5	16.7%	49.2	122	91.8%	209.6	3.3%	46.0	59	62.7%	176.0	32.2%	67.1	0	0	0	0	0
	7	1716	25.6%	134.2	21.2%	51.8	3681	54.2%	165.6	22.5%	56.9	1356	33.8%	141.8	12.9%	46.7	577	43.5%	153.7	8.8%	49.5
	8	1188	18.9%	118.5	6.9%	33.1	2805	35.3%	143.1	14.7%	44.0	1671	18.9%	121.2	10.1%	42.5	1268	31.9%	144.3	6.0%	39.7
	6~8	9320	46.6%	158.6	16.3%	47.6	365	54.2%	169.8	18.8%	51.2	3086	26.3%	131.3	11.7%	44.8	1845	35.5%	147.3	6.9%	42.8
YRD	6	19329	26.2%	127.2	4.4%	36.8	11098	14.3%	107.0	2.2%	44.5	181	12.7%	102.4	0.6%	32.0	0	0	0	0	0
	7	5207	24.5%	119.8	5.3%	38.6	8459	22.0%	120.1	0.6%	28.0	4135	14.5%	112.6	0.1%	24.0	1743	30.9%	139.5	0.3%	30.0
	8	3593	25.5%	127.6	0.3%	28.6	19922	18.3%	113.8	3.0%	33.3	4993	16.9%	116.7	0.0%	23.7	3817	14.7%	114.8	0.1%	25.1
	6~8	28129	25.8%	125.9	4.0%	36.1	13754	17.4%	112.5	1.7%	30.6	9309	15.8%	114.6	0.1%	24.0	5560	19.7%	122.5	0.1%	26.7
PRD	6	5327	5.2%	80.1	0	16.8	101	31.7%	146.9	0	24.9	48	0	77.6	0	13.2	0	0	0	0	0
	7	1431	20.3%	107.2	0.6%	25.3	3076	7.6%	81.8	0.1%	19.1	1079	13.3%	92.4	0	19.3	461	8.0%	82.1	0	17.9
	8	977	25.4%	122.5	1.1%	27.9	2316	20.6%	108.5	0.6%	28.0	1376	15.5%	103.4	0.3%	24.0	993	17.9%	111.4	0.1%	25.1
	6~8	7735	10.5%	90.5	0.2%	19.8	5493	13.5%	94.3	0.3%	23.0	2503	14.3%	98.2	0.2%	21.8	1454	14.8%	102.1	0.1%	22.8
GZP	6	1549	42.9%	147.6	0.4%	33.2	38	52.6%	165.3	0	30.4	19	26.3%	150.8	0	34.7	0	0	0	0	0
	7	1879	40.7%	145.0	1.9%	33.7	1168	47.4%	160.3	0	30.2	432	24.3%	133.3	1.2%	31.7	173	26.6%	144.1	0	26.4
	8	537	28.5%	134.0	1.6%	31.6	850	36.8%	146.3	1.6%	34.2	530	28.9%	143.1	1.9%	37.2	394	38.6%	154.9	1.3%	39.9
	6~8	368	15.2%	112.9	0.9%	32.4	2056	43.1%	154.6	2.1%	35.9	981	26.8%	138.9	1.5%	34.7	567	34.9%	151.6	0.9%	35.8
NEM	6	13126	17.9%	121.0	1.7%	26.4	243	64.2%	175.3	0.4%	31.1	120	13.3%	123.3	0.8%	37.6	0	0	0	0	0
	7	3422	8.9%	106.8	2.3%	25.2	7338	17.0%	120.7	1.3%	28.1	2722	5.7%	93.0	0.7%	20.8	1141	15.1%	122.4	0.2%	24.3
	8	2341	4.4%	92.6	1.0%	20.1	5520	6.3%	91.0	1.3%	21.0	3282	5.6%	98.3	0.9%	23.2	2507	7.8%	97.8	0.2%	19.5
	6~8	18889	14.6%	114.9	1.7%	25.4	13101	13.4%	109.2	1.3%	25.2	6124	5.8%	96.4	0.8%	22.4	3648	10.1%	105.5	0.2%	21.0

Notes: stas × days, stations × days; OLR, Over-limit ratio; Con, Concentration (μg m^{-3}).

https://doi.org/10.5194/acp-2020-596
Preprint. Discussion started: 6 August 2020

Atmospheric Chemistry and Physics Discussions

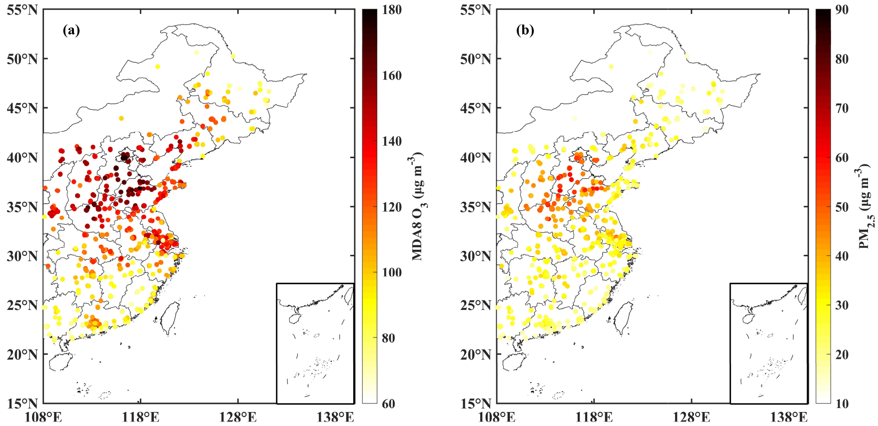

Fig. 1. Average concentration of MDA8 O_3 (a) and $PM_{2.5}$ (b) in eastern China during summers of 2015–2018. Stations and key urban clusters (red box) are shown in (a).

https://doi.org/10.5194/acp-2020-596
Preprint. Discussion started: 6 August 2020

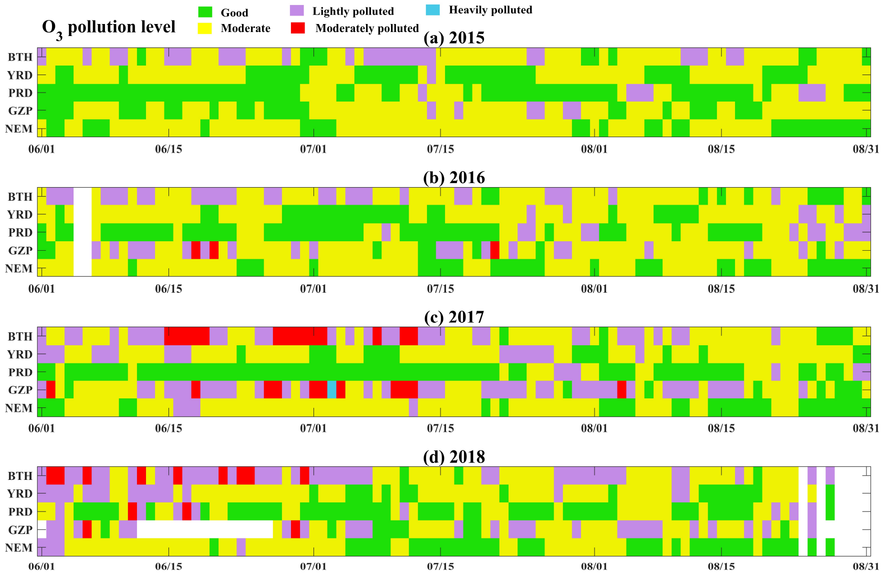

685 **Fig. 2. Time series of MDA8 O_3 pollution levels in key urban clusters.**

https://doi.org/10.5194/acp-2020-596
Preprint. Discussion started: 6 August 2020

Atmospheric Chemistry and Physics Discussions

Fig.3. Time series of $PM_{2.5}$ pollution levels in key urban clusters.

690

https://doi.org/10.5194/acp-2020-596
Preprint. Discussion started: 6 August 2020

Atmospheric Chemistry and Physics Discussions
Open Access

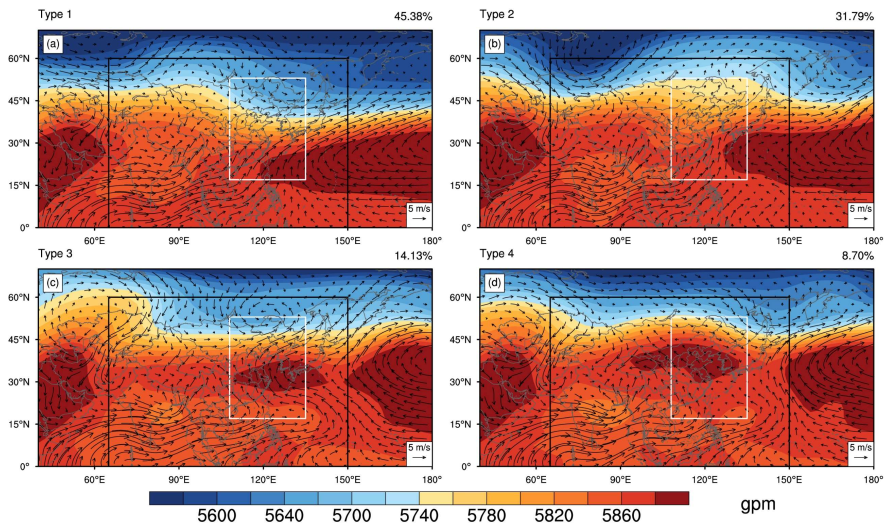

Fig. 4. 850-hPa wind (vectors; see scale arrow at the bottom right in units of 5m/s) and 500-hPa GH (contours; see scale bar at bottom in units of gpm) patterns based on objective classification (see text for details). Black box area indicates the area for classification and the white box area is for the area of eastern China, the number at the upper right corner of each panel indicates the frequency of the occurrence of each pattern type.

https://doi.org/10.5194/acp-2020-596
Preprint. Discussion started: 6 August 2020

Atmospheric Chemistry and Physics
Discussions

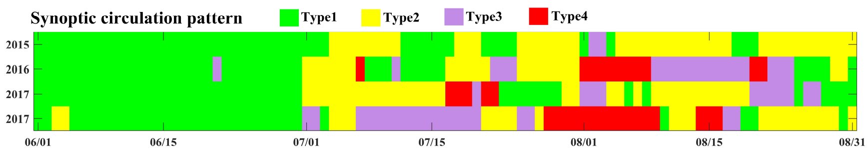

Fig. 5. Time series of synoptic circulation pattern.

https://doi.org/10.5194/acp-2020-596
Preprint. Discussion started: 6 August 2020

Atmospheric Chemistry and Physics
Discussions

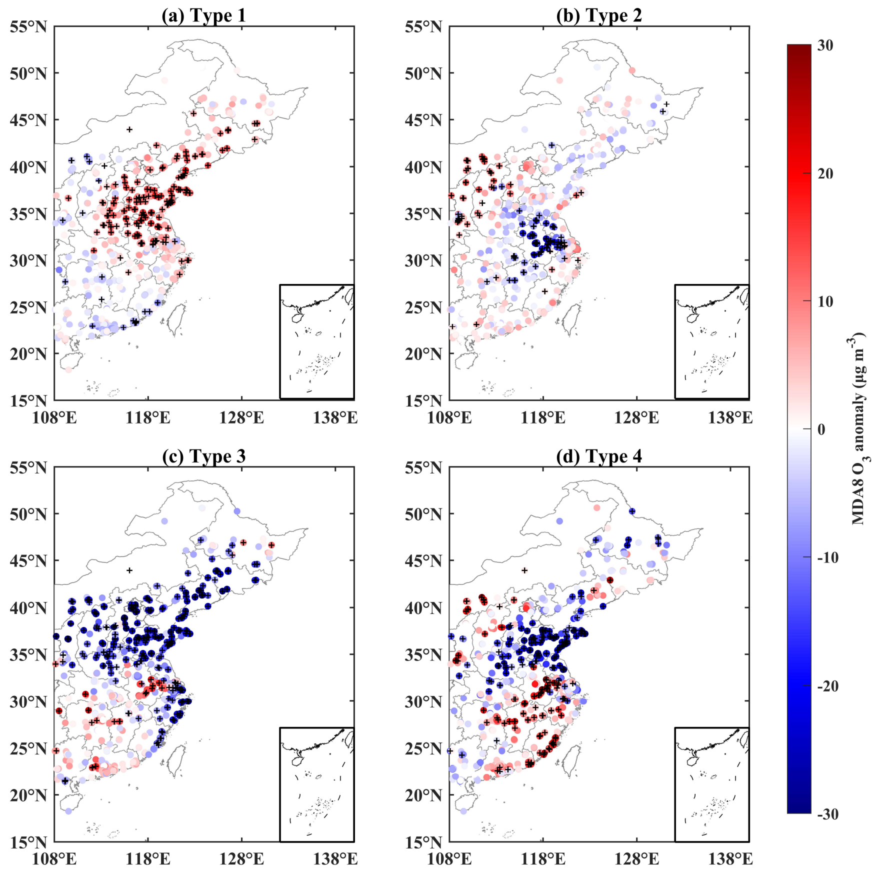

Fig. 6. The MDA8 O_3 anomaly under four SWPs, where the sites marked with a '+' indicates the Analysis of Variance passes the significance level of 0.05.

https://doi.org/10.5194/acp-2020-596
Preprint. Discussion started: 6 August 2020

Atmospheric Chemistry and Physics
Discussions

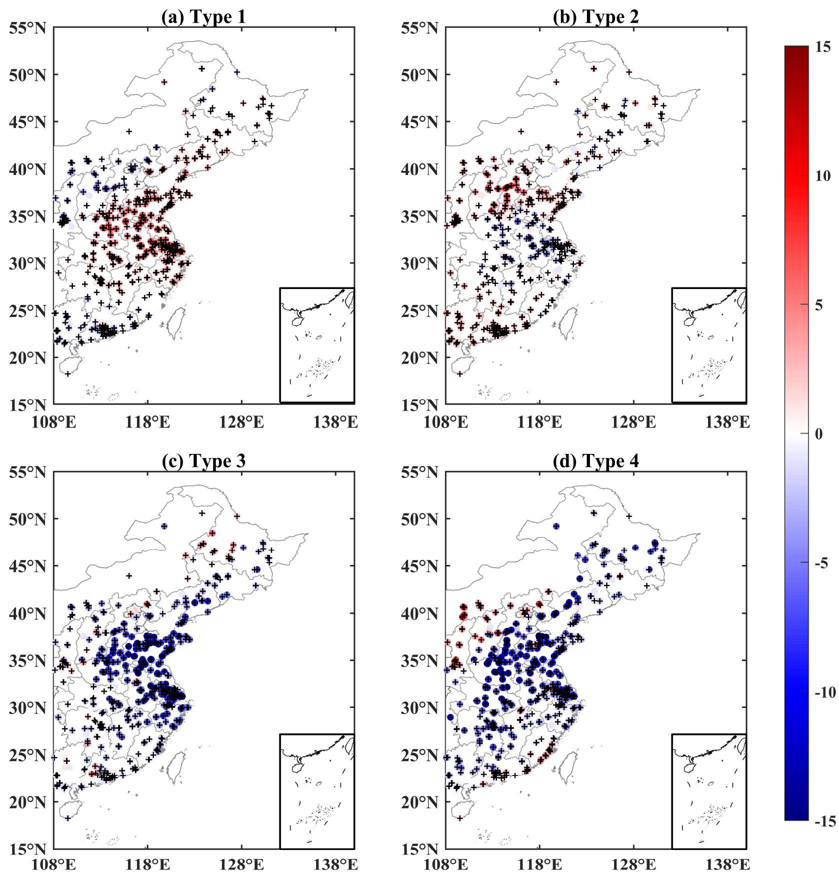

705

Fig. 7. The $PM_{2.5}$ anomaly under four SWPs, where the sites marked with a '+' indicates the Analysis of Variance passes the significance level of 0.05.

https://doi.org/10.5194/acp-2020-596
Preprint. Discussion started: 6 August 2020

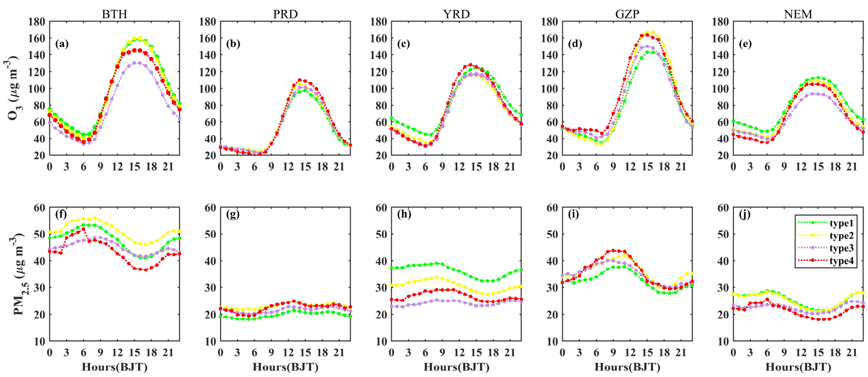

710 **Fig. 8. Daily variation of O_3 and $PM_{2.5}$ under four SWPs in key urban clusters.**

https://doi.org/10.5194/acp-2020-596
Preprint. Discussion started: 6 August 2020

Atmospheric Chemistry and Physics
Open Access
Discussions

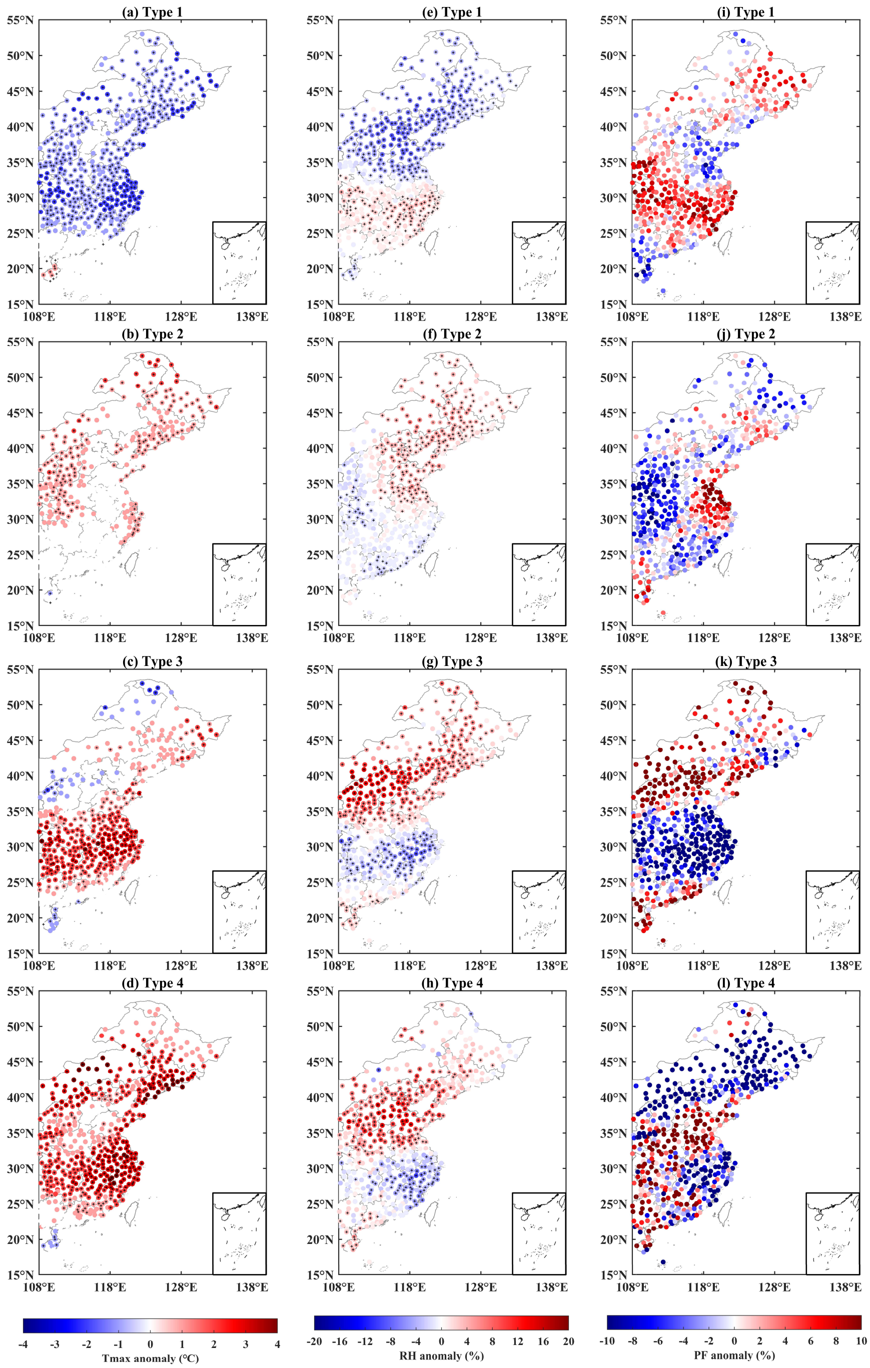

Fig. 9. The anomaly of Tmax (a–d), RH (e–h), and PF (i–l) under four SWPs, where the sites marked with a '+' indicates the Analysis of Variance passes the significance level of 0.05.

https://doi.org/10.5194/acp-2020-596
Preprint. Discussion started: 6 August 2020

Atmospheric Chemistry and Physics Discussions

715 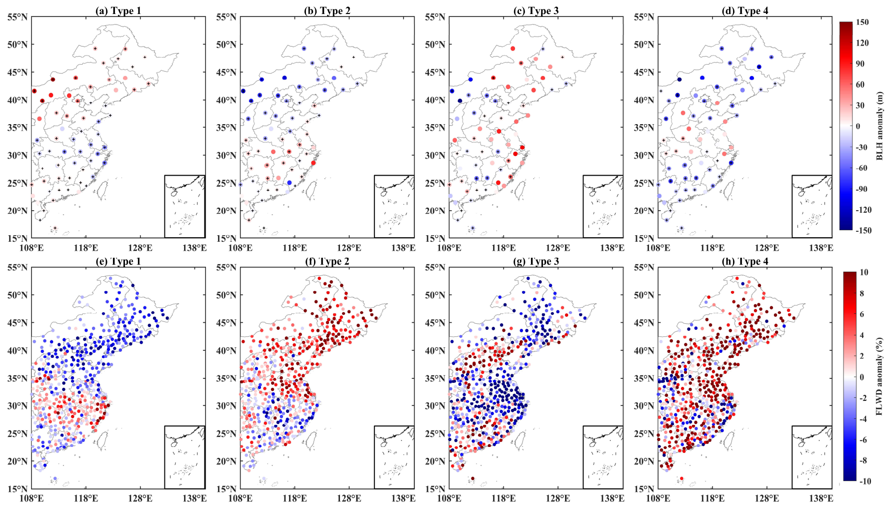

Fig. 10. The anomaly and significance of difference of BLH (a–d) and FLWD (e–h) under four SWPs, where the sites marked with a '+' indicates the Analysis of Variance passes the significance level of 0.05.

https://doi.org/10.5194/acp-2020-596
Preprint. Discussion started: 6 August 2020

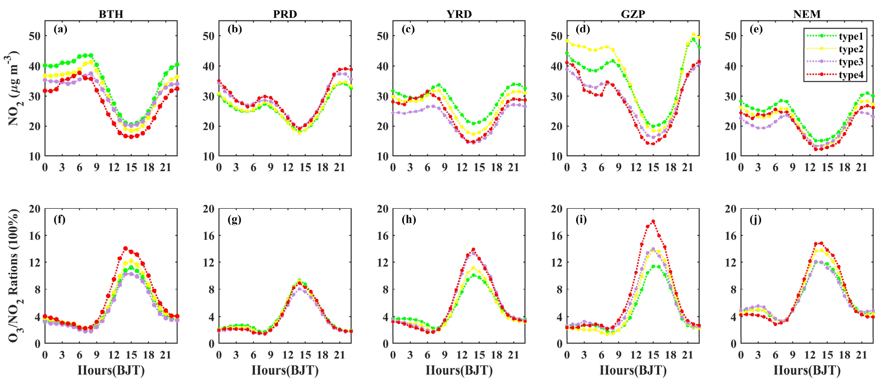

720

Fig. 11. NO_2 and O_3/NO_2 daily variation under four SWPs in key urban clusters.

https://doi.org/10.5194/acp-2020-596
Preprint. Discussion started: 6 August 2020

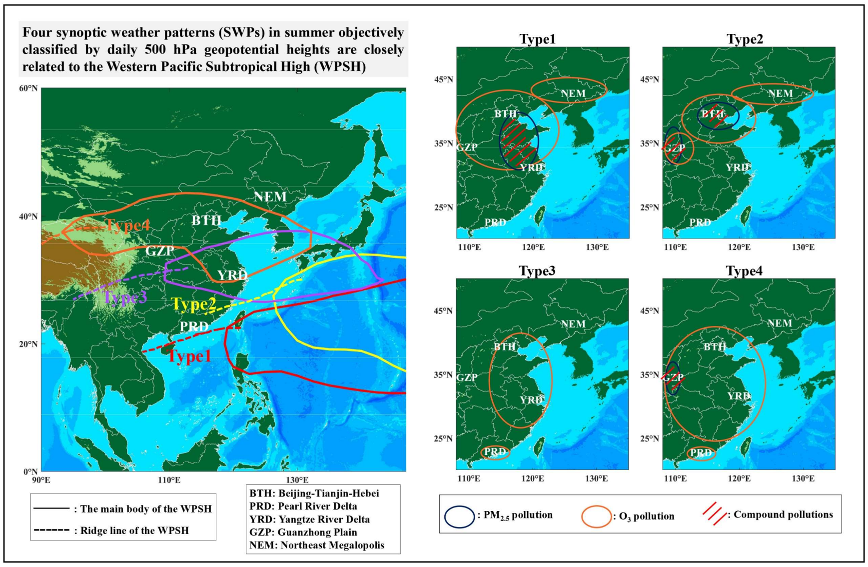

Fig. 12. Schematic diagrams describing the relationships between the WPSH, four SWPs and

725 **summertime O_3 and $PM_{2.5}$ pollution in various regions.**